The 8th European Congress on Computational Methods in Applied Sciences and Engineering
ECCOMAS Congress 2022
5 – 9 June 2022, Oslo, Norway

COUPLED THERMOMECHANICAL ANALYSIS OF THERMOPLASTIC COMPOSITE PIPE BY FEM SIMULATIONS

IGOR A. GUZ[*], JAMES C. HASTIE[†] AND MARIA KASHTALYAN[†]

[*]School of Engineering and Physical Sciences
Heriot-Watt University, Edinburgh EH14 4AS, Scotland, U.K.
e-mail: i.guz@abdn.ac.uk

[†] Centre for Micro- and Nanomechanics (CEMINACS), School of Engineering
University of Aberdeen, Scotland, U.K.
e-mail: m.kashtalyan@abdn.ac.uk

Key words: Thermoplastic Composite Pipes, Finite Element Analysis, Coupled Thermomechanical Analysis, Lamina Failure Criteria.

Abstract. Spoolable thermoplastic composite pipe (TCP) is an ideal alternative to traditional, heavier metallic counterparts for deepwater riser applications. During operation the pipe is subjected to mechanical loads simultaneously with through-wall thermal gradients arising from the mismatch between temperatures of hot pipe contents and cool surrounding ocean. In this work, structural analysis of TCP under coupled thermomechanical loads is performed using the finite element method (FEM). Temperature-dependent material properties are considered. Material safety factors for different laminate stacking sequences are compared and multi-angle stacking is shown to be effective for both pressure- and tension-dominated scenarios. Safety factors are also generated for TCP bent at reduced and elevated temperatures illustrative of spooling in different environments. It is clear that optimising the laminate for operation will adversely affect spooling capacity and vice-versa, i.e. TCP intended for extreme in-service conditions will require large spools.

1 INTRODUCTION

Thermoplastic composite pipe (TCP), consisting of fibre-reinforced thermoplastic laminate sandwiched between unreinforced thermoplastic liners (Figure 1), is a lightweight spoolable pipe solution ideal for riser applications in deep waters where the weight of metallic counterparts becomes problematic. Acceptance of composite materials in the offshore industry was historically hindered by a reluctance to use materials widely regarded as "complex". Lacks of performance data and regulatory requirements, intricate design procedures and repairability issues have previously been seen as factors preventing wide acceptance [1]. However, the spotlight has shifted to lightweight fibre-reinforced plastic (FRP) solutions in recent years as exploration and production continues to extend globally into deeper waters and harsher environments. Uptake has accelerated with the advent of an industry standard for TCP design, DNVGL-ST-F119, developed with input from leading manufacturers [2].

TCP is subjected to mechanical loading in conjunction with temperature profiles including through-wall thermal gradients that arise when operating in deep, cold waters with hot pipe contents. Experimental work on combined thermal and mechanical loading of FRP tubulars is largely limited to pressure [3,4] or tensile [5] tests performed at different controlled temperatures, which have generally revealed strength reductions at high temperatures and strong dependence on fibre angle. In lieu of experimental programs, researchers have studied the behaviour of multi-layered tubulars comprising isotropic layers [6], FRP layers [7] or a combination of both (as in composite sandwich pipe) [8] under combined pressure and varying through-thickness temperature profiles using analytical or numerical approaches. Numerical models developed using dedicated finite element (FE) software afford the ability to introduce a variety of loads simultaneously once a base model is established. Furthermore, the inclusion of pipe defects is possible where this may prove highly complex or unfeasible to accomplish within an analytical framework.

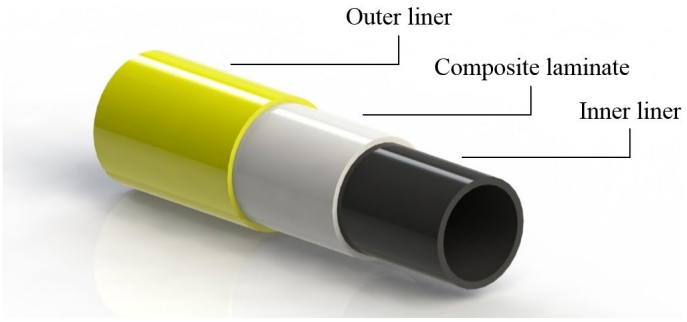

Figure 1: TCP construction

In previous works by the authors, a 3D FE model was developed for stress analysis of TCP subjected to combined pressures, tension and thermal gradient illustrative of deepwater single-leg hybrid riser (SLHR) operation, accounting for temperature-dependent material properties [9-11]. Failure indices based on Maximum Stress, Tsai-Hill and Hashin criteria have been compared for angle-ply and multi-angle laminate configurations under varying load combinations. The case of TCP bending at reduced and elevated temperatures, representative of spooling onto a storage drum in extreme environments, has also been investigated by coupled thermomechanical FE modelling [12]. In the present paper, stresses obtained from FE simulations are used to evaluate material safety factors, in line with industry guidelines, for TCP subjected to operating and spooling loads. Various laminate stacking sequences are considered.

2 FINITE ELEMENT MODELS

2.1 Operating model

An FE model for stress analysis of a section of TCP under SLHR loads was developed in Abaqus/CAE for previous studies on TCP failure response [9-11]. The model is shown in Figure 2. Internal and external pressures (P_i and P_e) are applied on the surfaces and axial tension (F_z) is applied using a reference point and kinematic coupling at one end, with the other end restrained. In the same step the internal surface temperature (T_i) is applied as a

boundary condition and on the external surface a film condition is defined to simulate convection based on surrounding temperature, T_∞, and heat transfer coefficient, h. A reference temperature, T_{ref}, is defined in the initial step using a predefined field. The model is meshed using the reduced-integration, thermally coupled, 20-node element type C3D20RT available in Abaqus.

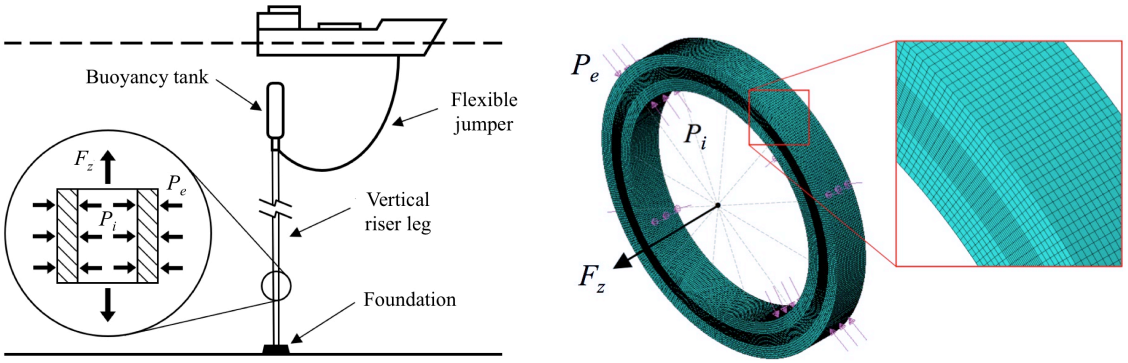

Figure 2: Operating model

2.2 Spooling model

A combined bending and uniform thermal load model was developed in an earlier study [12]. The model and end constraints are shown in Figure 3; the model is meshed using C3D20RT elements. Bending is imposed via rotation, ur_X, applied to reference points located at the centre of each end and coupled to the corresponding end nodes. The total angle of rotation is L/R, where L is the length of the section and R is the bending radius. Uniform temperature, T, is applied as a boundary condition to the entire section in the same step. A pre-defined field is used to define the initial temperature.

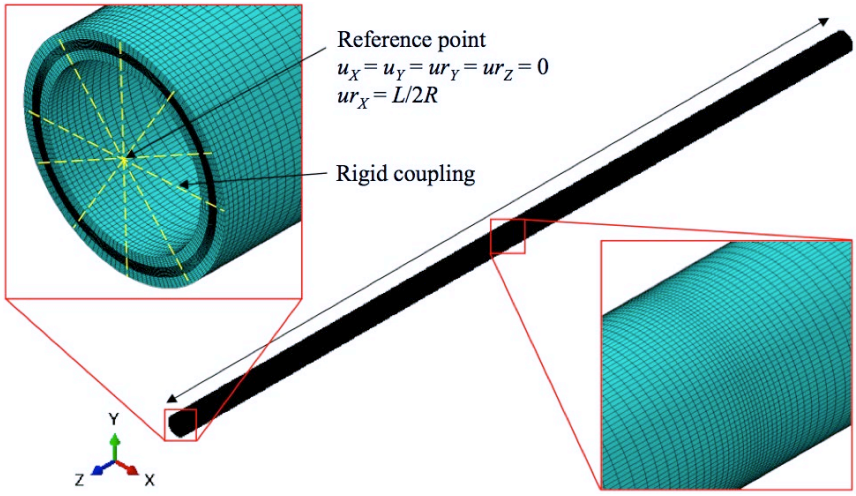

Figure 3: Spooling model (end constraints symmetrical at opposite end)

2.3 Pipe configuration and materials

The pipe dimensions studied here resemble real-world products without emulating any one

in particular. Internal and external radii are 76 mm and 100 mm respectively. The inner liner, FRP laminate and outer liner are each 8 mm thick. The laminate comprises eight 1 mm-thick unidirectional layers. Four configurations with different unidirectional layer orientations are studied. These are summarised in Table 1. The pipe consists of unidirectional AS4/APC-2 carbon/PEEK layers and unreinforced APC-2 PEEK liners. Temperature-dependent material properties are listed in Hastie et al. [9].

Table 1: TCP laminate sequences

TCP	Stacking sequence
A	$[\pm 55]_4$
B	$[\pm 42.5]_4$
C	$[\pm 30]_4$
D	$[(\pm 55)_2/(\pm 30)_2]$

3 FAILURE ANALYSIS

The analysis of liner and laminate material failures in line with DNVGL-ST-F119 [2] is discussed in this section.

3.1 Failure criteria

Yielding of the ductile liners is evaluated according to the von Mises criterion:

$$\gamma_M \gamma_{Rd} \sqrt{\frac{(\sigma_1 - \sigma_2)^2 + (\sigma_2 - \sigma_3)^2 + (\sigma_3 - \sigma_1)^2}{2}} < \sigma_y \tag{1}$$

where σ_y is the yield strength; γ_{Rd} is the resistance model factor that depends on specific failure mechanisms ($\gamma_{Rd} = 1.0$ for yielding) [2]; γ_M is the material safety factor. Equation 1 can be rearranged to obtain γ_M under applied stress state.

Failure of fibre-reinforced layers considered brittle is evaluated according to a modified Maximum Stress criterion. The criterion for fibre failure is

$$\sigma_1 < \frac{X_T}{\gamma_M \gamma_{Rd}} \quad \text{if} \quad \sigma_1 > 0 \qquad |\sigma_1| < \frac{X_C}{\gamma_M \gamma_{Rd}} \quad \text{if} \quad \sigma_1 < 0 \tag{2}$$

where X_T and X_C are the strengths under tension and compression respectively along the fibre direction. A model factor of $\gamma_{Rd} = 1.0$ is taken for fibre failure.

Matrix cracking is assumed to occur when the material strength in any other principal direction is exceeded. The design criterion takes different forms depending on whether a single stress is dominating. A stress is dominating if the following is satisfied:

$$\left(\max\left(\frac{|\sigma_i|}{\sigma_i^u}, \frac{|\tau_j|}{\tau_j^u} \right) \right) \Big/ \left(\sum_i \left(\frac{|\sigma_i|}{\sigma_i^u} \right) + \sum_j \left(\frac{|\tau_j|}{\tau_j^u} \right) - \max\left(\frac{|\sigma_i|}{\sigma_i^u}, \frac{|\tau_j|}{\tau_j^u} \right) \right) \geq 10 \tag{3}$$

where $i = 2, 3$ and $j = 23, 13, 12$. The characteristic strengths σ_i^u depend on the stress signs:

$$\begin{aligned} \sigma_2^u &= Y_T \quad \text{if} \quad \sigma_2 > 0 \qquad \sigma_2^u = Y_C \quad \text{if} \quad \sigma_2 < 0 \\ \sigma_3^u &= Z_T \quad \text{if} \quad \sigma_3 > 0 \qquad \sigma_3^u = Z_C \quad \text{if} \quad \sigma_3 < 0 \end{aligned} \tag{4}$$

where Y and Z are the strengths in tension or compression (subscripts 'T' and 'C') in principal

directions 2 and 3 respectively; the shear strengths, τ_f^u, are sign-independent. In the case of a dominating stress the safe limits for matrix cracking are

$$|\sigma_2| < \frac{\sigma_2^u}{\gamma_M \gamma_{Rd}} \qquad |\sigma_3| < \frac{\sigma_3^u}{\gamma_M \gamma_{Rd}}$$
$$|\tau_{23}| < \frac{\tau_{23}^u}{\gamma_M \gamma_{Rd}} \qquad |\tau_{13}| < \frac{\tau_{13}^u}{\gamma_M \gamma_{Rd}} \qquad |\tau_{12}| < \frac{\tau_{12}^u}{\gamma_M \gamma_{Rd}} \tag{5}$$

The resistance model factor is taken as $\gamma_{Rd} = 1.0$ for the dominating case. If Equation 3 is not satisfied, the matrix criterion takes a modified form to account for stress interactions:

$$\gamma_M \gamma_{Rd} \sqrt{\left(\frac{\sigma_2}{\sigma_2^u}\right)^2 + \left(\frac{\sigma_3}{\sigma_3^u}\right)^2 + \left(\frac{\tau_{23}}{\tau_{23}^u}\right)^2 + \left(\frac{\tau_{13}}{\tau_{13}^u}\right)^2 + \left(\frac{\tau_{12}}{\tau_{12}^u}\right)^2} < 1 \tag{6}$$

A factor of $\gamma_{Rd} = 1.15$ is used to ensure a conservative result for the simplified treatment of component interactions.

3.2 Safety classes

Acceptable safety factors depend on the coefficient of variation (COV) for the material and whether failure is ductile (liner yielding) or brittle (FRP layer failure, which demands higher safety factors). The COV is calculated using the standard deviation and mean value of strengths determined by specimen tests, as defined in DNVGL-ST-F119 [2]. Low, medium and high safety factor classifications for functional loading as per DNVGL-ST-F119 are given in Table 2 for 5 % and 12.5 % COV. In addition to the safety classes, two types of failure are distinguished in this study. These are failure of the material (i.e. safety factor ≤ 1.0) or safety class failure (factor > 1.0 but below lower limit of low safety class). Safety factor for the FRP laminate is taken as the minimum value of γ_M corresponding to any layer. Classifications for the special case of spooling are listed in Table 3.

Table 2: Material safety factors for functional loads

Classification	**Liners (ductile)**		**FRP layers (brittle)**	
	5 % COV	**12.5 % COV**	**5 % COV**	**12.5 % COV**
Failure (material)	$\gamma_M \leq 1.0$	$\gamma_M \leq 1.0$	$\gamma_M \leq 1.0$	$\gamma_M \leq 1.0$
Failure (safety class)	$1.0 < \gamma_M < 1.2$	$1.0 < \gamma_M < 1.1$	$1.0 < \gamma_M < 1.3$	$1.0 < \gamma_M < 1.3$
Safety class – low	$1.2 \leq \gamma_M < 1.3$	$1.1 \leq \gamma_M < 1.3$	$1.3 \leq \gamma_M < 1.45$	$1.3 \leq \gamma_M < 1.5$
Safety class – medium	$1.3 \leq \gamma_M < 1.45$	$1.3 \leq \gamma_M < 1.5$	$1.45 \leq \gamma_M < 1.6$	$1.5 \leq \gamma_M < 1.75$
Safety class – high	$\gamma_M \geq 1.45$	$\gamma_M \geq 1.5$	$\gamma_M \geq 1.6$	$\gamma_M \geq 1.75$

Table 3: Material safety factors for spooling

Classification	**Liners (ductile)**		**FRP layers (brittle)**	
	5 % COV	**12.5 % COV**	**5 % COV**	**12.5 % COV**
Failure (material)	$\gamma_M \leq 1.0$	$\gamma_M \leq 1.0$	$\gamma_M \leq 1.0$	$\gamma_M \leq 1.0$
Failure (safety class)	$1.0 < \gamma_M < 1.2$	$1.0 < \gamma_M < 1.3$	$1.0 < \gamma_M < 1.2$	$1.0 < \gamma_M < 1.5$
Safety class – low	-	$1.3 \leq \gamma_M < 1.5$	$1.2 \leq \gamma_M < 1.3$	$1.5 \leq \gamma_M < 1.7$
Safety class – medium	$1.2 \leq \gamma_M < 1.3$	$1.5 \leq \gamma_M < 1.7$	-	$1.7 \leq \gamma_M < 1.9$
Safety class – high	$\gamma_M \geq 1.3$	$\gamma_M \geq 1.7$	$\gamma_M \geq 1.3$	$\gamma_M \geq 1.9$

4 RESULTS AND DISCUSSION

4.1 Operation

TCP subjected to various combinations of pressure, axial tension and through-thickness thermal gradient illustrative of SLHR operation is firstly investigated. Two external pressures, P_e = 10 MPa and 30 MPa (corresponding to roughly 1,000 m and 3,000 m ocean depths), are considered here. These are applied in combination with internal pressure, $P_i = 1.5P_e$ or $2P_e$, and axial tension, F_z = 50 kN or 500 kN. In all cases an internal surface temperature of T_i = 130 °C is applied and the outer surface is exposed to T_∞ = 4 °C with heat transfer coefficient of h = 50 $Wm^{-2}°C^{-1}$. An initial temperature of T_{ref} = 23 °C is assumed.

Liner and laminate safety factors for the four configurations are presented in Table 4 and Table 5 for the P_e = 10 MPa cases. The safety classes are colour coded according to Table 2 for the largest COV (12.5 %) considered in DNVGL-ST-F119 for conservativeness since test specimen data was not available for the compiled temperature-dependent strengths used here (i.e. a COV could not be obtained). The liners exhibit lower safety factor than the FRP layers. It has previously been shown that the inner liner is particularly sensitive to high operating temperatures [9-11]. Higher safety factor for composite layers is desirable when one considers their load-bearing role and the inherently greater uncertainty in heterogeneous failure modelling. Furthermore, yielding of the liners that serve as protective/sealing barriers does not necessarily constitute a loss of function.

The laminates mostly qualify as high safety. In all cases matrix failure is found to be more critical than fibre failure and was evaluated according to Equation 6 since the condition for a dominating stress (Equation 3) was not satisfied. The TCP A laminate with highest fibre angle (55°) performs better under lower tension, while conversely TCP C with lowest fibre angle (30°) performs better under high tension. TCP B with 42.5° fibre orientation exhibits reasonably consistent laminate safety factor under pressure- or tension-dominated loading, as does TCP D comprising both 55° and 30° layers.

Table 4: Liner material safety factors: P_e = 10 MPa (12.5 % COV classes)

Loads		**Liner safety factors**			
F_z **(kN)**	P_i **(MPa)**	**TCP A**	**TCP B**	**TCP C**	**TCP D**
50	15	1.247	1.245	1.468	1.230
	20	1.397	1.420	1.631	1.435
500	15	1.227	1.189	1.477	1.295
	20	1.504	1.610	2.088	1.634

Table 5: FRP laminate material safety factors: P_e = 10 MPa (12.5 % COV classes)

Loads		**FRP laminate safety factors**			
F_z **(kN)**	P_i **(MPa)**	**TCP A**	**TCP B**	**TCP C**	**TCP D**
50	15	6.706	6.746	4.397	6.763
	20	5.825	4.246	2.045	5.106
500	15	1.730	4.532	7.682	6.143
	20	1.902	5.810	2.631	5.927

Safety factors for the P_e = 30 MPa scenarios are given in Table 6 and Table 7. Again, the interactive matrix failure mode is dominant for all laminates. In general, safety factors for liners and laminates are higher and lower respectively than those for the corresponding P_e = 10 MPa cases, i.e. higher pressure creates a trade-off between better margin of safety for the liner but greater utilisation of the laminate. A notable exception is TCP C subjected to P_i = 60 MPa; the liners and laminate are expected to fail as a result of insufficient hoop reinforcement to handle large pressure. The TCP B liner also does not qualify in line with the standard under P_i = 60 MPa, F_z = 50 kN. As per the P_e = 10 MPa cases, the TCP D laminate is consistently high safety and therefore demonstrates suitability for varying pressure and tension scenarios.

Table 6: Liner material safety factors: P_e = 30 MPa (12.5 % COV classes)

Loads		**Liner safety factors**			
F_z **(kN)**	P_i **(MPa)**	**TCP A**	**TCP B**	**TCP C**	**TCP D**
50	45	2.370	2.137	1.751	2.262
	60	2.710	1.028	0.644	1.748
500	45	1.704	2.747	2.865	2.874
	60	3.268	1.715	0.748	2.899

Table 7: FRP laminate material safety factors: P_e = 30 MPa (12.5 % COV classes)

Loads		**FRP laminate safety factors**			
F_z **(kN)**	P_i **(MPa)**	**TCP A**	**TCP B**	**TCP C**	**TCP D**
50	45	2.811	2.624	1.718	2.735
	60	2.043	1.412	0.696	1.872
500	45	1.619	2.812	2.110	2.852
	60	1.935	1.720	0.766	2.073

4.2 Spooling

Bending of TCP at low and high temperatures representative of spooling in different thermal settings is now investigated. In a preceding work it was shown that orientating unidirectional layers at an ‘intermediate’ fibre angle is superior to orientating layers at high or low angles relative to the pipe longitudinal axis which results in large transverse or fibre stresses respectively under bending [12]. In practical terms, TCP B with 42.5° angle-ply stacking sequence outperforms 55° (TCP A) and 30° (TCP C) counterparts in the case of spooling. Multi-angle stacks combining both high and low angles are also inferior due to large fibre stresses manifesting in the low angle layers.

Here, practical minimum bending radii are assessed for optimal and sub-optimal configurations. The variation of TCP A and B laminate safety factors with bending radius at T = 0 °C and 50 °C is shown in Figure 4. The plots are overlaid onto the classes for a conservative COV of 12.5 % (class envelopes are lightly shaded according to the colours in Table 3). The TCP A laminate does not qualify in the bracket of lowest acceptable safety at either temperature. Bending of TCP B to relatively large radius of R = 10 m is acceptable at T = 0 °C although with very little leeway. At T = 50 °C the laminate can be bent to approximately R = 9 m and comply with the regulation.

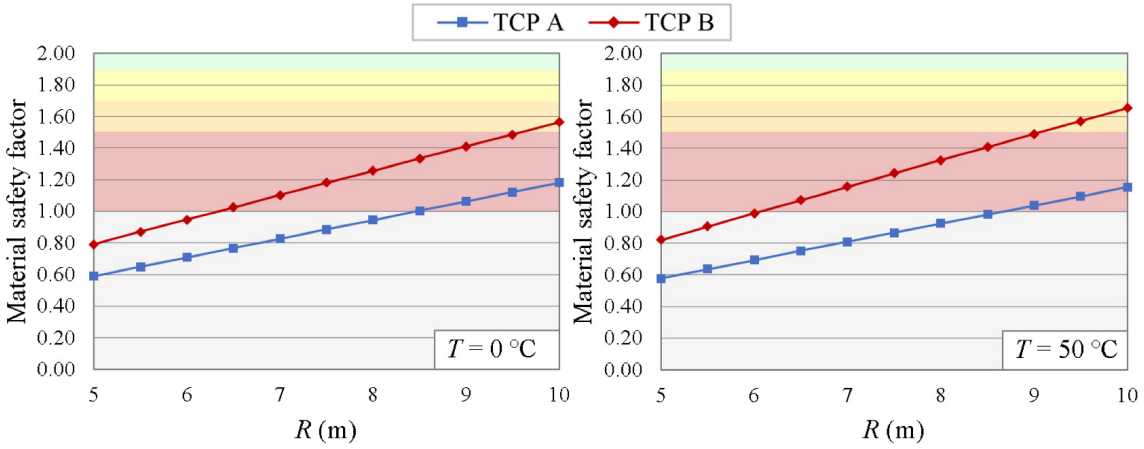

Figure 4: FRP laminate material safety factor vs. bending radius at temperature (12.5 % COV classes)

In Figure 5, the plots are overlaid onto safety classes based on smaller COV of 5 %, i.e. assuming greater consistency in material test data. The factor for the TCP A laminate remains below the bottom limit of the lowest safety class and therefore the configuration would not qualify according to DNVGL-ST-F119 for the range of bending considered here. TCP B is acceptable when bent down to roughly R = 7.5 m. The laminate qualifies as high safety for $R \geq 8.5$ m at T = 0 °C and $R \geq 8$ m at T = 50 °C. This is a considerable improvement in comparison to COV of 12.5 % and demonstrates the practical importance of material quality and achieving repeatability when obtaining the material data.

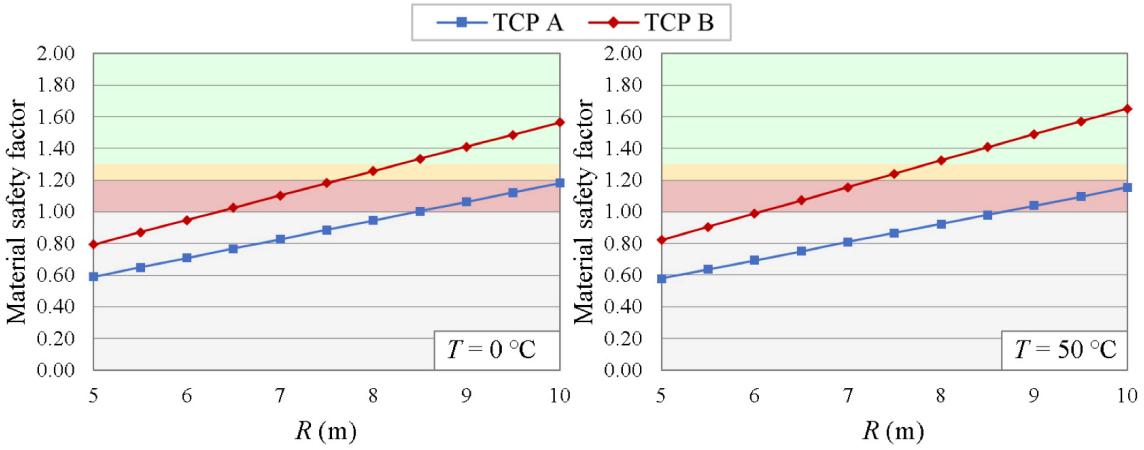

Figure 5: FRP laminate material safety factor vs. bending radius at temperature (5 % COV classes)

We finish by examining the thermoplastic liners. Minimum safety factors (of both inner and outer liner) are shown in Figure 6 and Figure 7 for high and low COV. The liners qualify easily for spooling at T = 0 °C based on COV of 12.5 %. A minimum bend radius of R = 6.5 m and 7 m is required for TCPs A and B respectively for basic acceptance at T = 50 °C. At the same temperature, these radii are considered highly safe according to the rules for 5 % COV, which again emphasises the benefit of reliable material data with low variation. Assuming 5 % COV the liners are considered high safety at T = 0 °C.

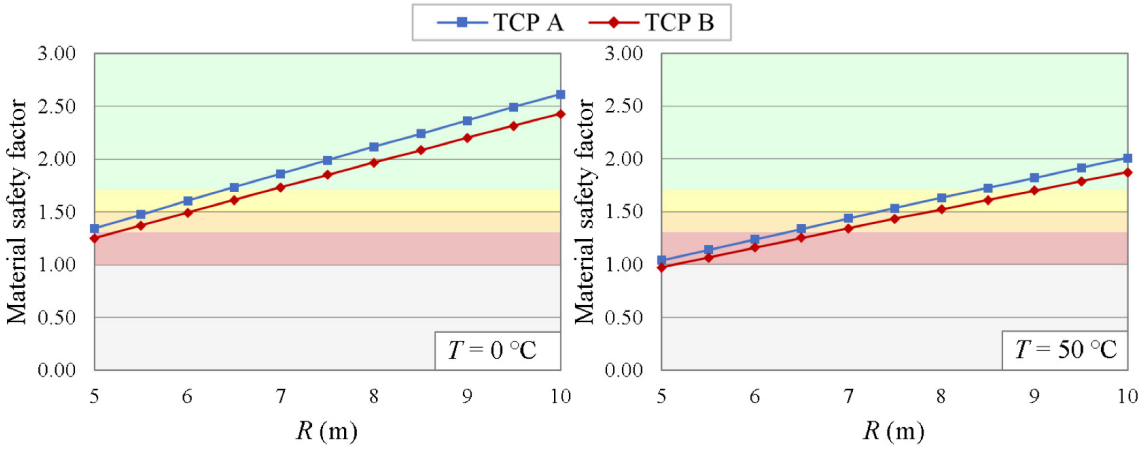

Figure 6: Liner material safety factor vs. bending radius at temperature (12.5 % COV classes)

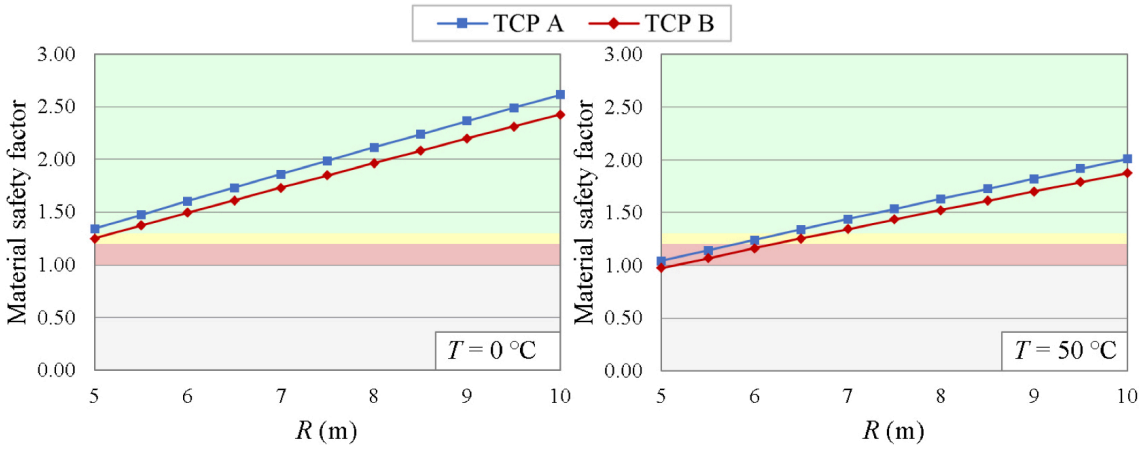

Figure 7: Liner material safety factor vs. bending radius at temperature (5 % COV classes)

4.3 Discussion

It is evident that optimisation of laminate stacking sequence for spooling will have implications on the performance of TCP when deployed in operation and subjected to different loads. Thus, both spooling and operating stages must be carefully considered in conjunction during the design phase. The multi-angle $[(\pm 55)_2/(\pm 30)_2]$ laminate is shown to be suitable for varying combinations of pressure and tension, while the $[\pm 42.5]_4$ stack is ideal for spooling. Large spooling radii may unavoidably be required for the storage and transportation of TCP designed to operate under the most extreme in-service conditions. This is compounded by the fact the spools must have sufficient volume to store very long pipe lengths intended for deep waters. Sizeable spools will have a direct bearing on installation procedures, vessel sizes and ancillary equipment but are not necessarily disconcerting given that the offshore installation of TCP is characteristically more economical than that of heavier metallic pipes. Nevertheless, vessel and accompanying equipment requirements must be factored into offshore deployment plans.

As is clear from the previous subsection, permissible spooling radii in line with current industry guidance is extremely sensitive to variation in material testing data. The need for

large spooling radii can be alleviated somewhat by consistent and reliable material testing, as well as continual improvements in composite material quality.

5 CONCLUSIONS

In this work, the behaviour of TCP under coupled thermal and mechanical loading was investigated by FE modelling. Material safety factors were assessed for configurations with different stacking sequences subjected to deepwater operating and spooling loads. Optimising the laminate for operation will adversely affect spooling capacity and vice-versa, thus large spools may invariably be required for TCP intended for extreme in-service conditions. Future work can be aimed at scrutinising the physical accuracy of lamina failure criteria with a view to reducing the required safety factors specified in current design guidelines.

REFERENCES

[1] Guz, I.A., Menshykova, M. and Paik, J.K. Thick-walled composite tubes for offshore applications: an example of stress and failure analysis for filament-wound multi-layered pipes. *Ships Offshore Struc.* (2017) **12(3)**:304-322.

[2] DNV GL. Standard DNVGL-ST-F119 Thermoplastic composite pipes (2018).

[3] Onder, A., Sayman, O., Dogan, T. and Tarakcioglu, N. Burst failure load of composite pressure vessels. *Compos. Struct.* (2009) **89(1)**:159-166.

[4] Sayman, O., Deniz, M.E., Dogan, T. and Yaylagan, E. Failure pressures of composite cylinders with a plastic liner. *J. Reinf. Plast. Comp.* (2011) **30(10)**:882-888.

[5] Ortenzi, A., de Carvalho, J. and Corvi, A. Comparison behavior of tensile tests for GFRP filament wound pipes with two different sectional areas regarding high temperature. *OMAE 2012* (2012). Rio de Janeiro, Brazil, 1-6 July. ASME, 955-961.

[6] Zhang, Q., Wang, Z.W., Tang, C.Y., Hu, D.P., Liu, P.Q. and Xia, L.Z. Analytical solution of the thermo-mechanical stresses in a multilayered composite pressure vessel considering the influence of the closed ends. *Int. J. Press. Ves. Pip.* (2012) **98**:102-110.

[7] Bakaiyan, H., Hosseini, H. and Ameri, E. Analysis of multi-layered filament-wound composite pipes under combined internal pressure and thermomechanical loading with thermal variations. *Compos. Struct.* (2009) **88(4)**:532-541.

[8] Hastie, J.C., Kashtalyan, M. and Guz, I.A. Analysis of filament-wound sandwich pipe under combined internal pressure and thermal load considering restrained and closed ends. *Int. J. Press. Ves. Pip.* (2021) **191**:104350.

[9] Hastie, J.C., Guz, I.A. and Kashtalyan, M. Effects of thermal gradient on failure of a thermoplastic composite pipe (TCP) riser leg. *Int. J. Press. Ves. Pip.* (2019) **172**:90-99.

[10] Hastie, J.C., Kashtalyan, M. and Guz, I.A. Failure analysis of thermoplastic composite pipe (TCP) under combined pressure, tension and thermal gradient for an offshore riser application. *Int. J. Press. Ves. Pip.* (2019) **178**:103998.

[11] Hastie, J.C., Guz, I.A. and Kashtalyan, M. Structural integrity of deepwater composite pipes under combined thermal and mechanical loading. *Procedia Struct. Int.* (2020) **28**:850-863.

[12] Hastie, J.C., Guz, I.A. and Kashtalyan, M. Numerical modelling of spoolable thermoplastic composite pipe (TCP) under combined bending and thermal load. *Ships Offshore Struc.* (2021) DOI: 10.1080/17445302.2021.1958534.